

Top-quark pair production in association with a  $W$  or  $Z$   
boson with the ATLAS experimentSEBASTIAN HEER<sup>1</sup>, ON BEHALF OF THE ATLAS COLLABORATION*Physikalisches Institut  
Universität Bonn, 53115 Bonn, Germany*

The cross section of the  $t\bar{t}Z$  and  $t\bar{t}W$  processes are measured in a simultaneous fit using  $36.1 \text{ fb}^{-1}$  of proton-proton collisions at a centre of mass energy of  $\sqrt{s} = 13 \text{ TeV}$  recorded by the ATLAS detector at the LHC. The result is found to be  $\sigma_{t\bar{t}Z} = 0.95 \pm 0.08 \text{ (stat.)} \pm 0.10 \text{ (syst.) pb}$  and  $\sigma_{t\bar{t}W} = 0.87 \pm 0.13 \text{ (stat.)} \pm 0.14 \text{ (syst.) pb}$  and compatible with the Standard Model.

PRESENTED AT

11<sup>th</sup> International Workshop on Top Quark Physics  
Bad Neuenahr, Germany, September 16–21, 2018

---

<sup>1</sup>Supported by European Research Council grant ERC-CoG-617185.  
Copyright 2018 CERN for the benefit of the ATLAS Collaboration. CC-BY-4.0 license.

# 1 Introduction

The  $t\bar{t}Z$  and  $t\bar{t}W$  processes provide direct access to the weak couplings of the top quark. In addition, the two processes are often found to be a relevant background in searches involving final states with multiple leptons and  $b$ -quarks. Measurements of  $\sigma_{t\bar{t}Z}$  and  $\sigma_{t\bar{t}W}$  can be used to set constraints on the weak couplings of the quarks, as well as impose limits on possible beyond the Standard Model (BSM) effects. Previous measurements by the ATLAS and CMS experiments [1, 2] indicate agreement with the Standard Model [3, 4].

The dataset of  $36.1 \text{ fb}^{-1}$  of proton-proton collisions at a centre of mass energy of  $\sqrt{s} = 13 \text{ TeV}$ , collected in 2015 and 2016 by the ATLAS detector is analysed. Final states with two, three or four isolated prompt leptons are considered in the analysis. More details about the analysis can be found in Reference [5].

# 2 Analysis Overview

Separate analysis channels are defined to target the  $t\bar{t}Z$  and  $t\bar{t}W$  processes. Each channel is divided into multiple regions in order to enhance the sensitivity to the signal. Table 1 lists the analysis channels and the targeted decay modes of the  $t\bar{t}Z$  and  $t\bar{t}W$  processes.

Table 1: List of  $t\bar{t}W$  and  $t\bar{t}Z$  decay modes and analysis channels targeting them. The symbols  $b$  and  $\nu$  denote a  $b$ -quark or antiquark and neutrino or antineutrino, respectively [5].

Process	$t\bar{t}$ decay	Boson decay	Channel
$t\bar{t}W$	$(\ell^\pm \nu b)(q\bar{q}b)$	$\ell^\pm \nu$	$2\ell$ SS
	$(\ell^\pm \nu b)(\ell^\mp \nu b)$	$\ell^\pm \nu$	Trilepton
$t\bar{t}Z$	$(q\bar{q}b)(q\bar{q}b)$	$\ell^+ \ell^-$	$2\ell$ OS
	$(\ell^\pm \nu b)(q\bar{q}b)$	$\ell^+ \ell^-$	Trilepton
	$(\ell^\pm \nu b)(\ell^\mp \nu b)$	$\ell^+ \ell^-$	Tetralepton

The  $2\ell$ -OS channel targets the  $t\bar{t}Z$  process and is affected by large backgrounds from  $Z$ +jets or  $t\bar{t}$  production. In order to separate the signal from background in the most efficient way, Boosted Decision Trees (BDTs) are used. Three BDTs are constructed and trained in regions requiring at least 5 jets. The number of input variables varies between 14 and 17. The most important input variables are found to be the pseudorapidity of the dilepton system and the transverse momenta of all jets divided by the sum of their energies. Each signal region is divided into 19 equal sized

bins of the BDT discriminator. The normalization factors of the  $Z$ +jets background with one or two heavy flavour jets, labeled as  $Z+1HF$  and  $Z+2HF$ , are determined in the fit to data.

The  $2\ell$ -SS channel targets the  $t\bar{t}W$  process and uses a total of 12 signal and control regions, classified by information about the lepton flavour, total charge and  $b$ -jet multiplicity. The dominant background arises from fake leptons, which are estimated by the matrix method [6] and charge-flip leptons. The control regions are used in a fit to measure fake and real lepton efficiencies, as well as in the final fit to determine the signal cross sections, anticorrelating the fake lepton background with the signal process.

The regions in the  $3\ell$  channel are divided into two groups, depending on whether a pair of OSSF leptons whose invariant mass is within 10 GeV of the  $Z$  boson mass is present. The signal regions are further categorized based on jet and  $b$ -jet multiplicities. Four signal regions for each signal process are defined. The dominant backgrounds for the regions targeting  $t\bar{t}Z$  arise from diboson production and the production of single top quarks in association with a  $Z$  boson. A control region is used to determine the normalization of the  $WZ$  background in the fit to data. The dominant background for the regions targeting  $t\bar{t}W$  arises from fake leptons, which is estimated by the matrix method.

The  $4\ell$  channel targets the  $t\bar{t}Z$  process and uses four signal regions depending on the  $b$ -jet multiplicity and the flavour of the leptons from the  $t\bar{t}$  system. In addition, a control region is used to determine the normalization of the  $ZZ$  background in the fit to data. The dominant backgrounds arise from the diboson production, the production of a single top quark in association with a  $W$  and a  $Z$  boson, as well as fake leptons. The fake lepton background is estimated from simulation, applying scale factors obtained from a fit in control regions enriched by fake leptons.

### 3 Results

The  $t\bar{t}Z$  and  $t\bar{t}W$  cross sections are simultaneously extracted using a binned maximum-likelihood fit to the numbers of events in the dilepton, trilepton and tetralepton signal and control regions. In total, the fit includes 11 signal plus 2 control regions from the  $t\bar{t}Z$ , and 16 signal plus 12 control regions from the  $t\bar{t}W$  analysis. In all regions, good agreement between observed values and the expectation is observed. The normalization corrections for the  $WZ$  and  $ZZ$  backgrounds with respect to the predictions are obtained from the fit and found to be compatible with unity:  $0.91 \pm 0.10$  for the  $WZ$  background and  $1.11 \pm 0.17$  for the  $ZZ$  background. The normalizations of the  $Z+1HF$  and  $Z+2HF$  backgrounds are mainly constrained in the low BDT output bins of the opposite-sign dilepton channel signal regions, where the signal contamination is low. Their values are found to be  $1.19 \pm 0.25$

and  $1.09 \pm 0.13$ , respectively. The measured values of the cross sections from the combined fit are  $\sigma_{t\bar{t}Z} = 0.95 \pm 0.08$  (stat.)  $\pm 0.10$  (syst.) pb =  $0.95 \pm 0.13$  pb and  $\sigma_{t\bar{t}W} = 0.87 \pm 0.13$  (stat.)  $\pm 0.14$  (syst.) pb =  $0.87 \pm 0.19$  pb, assuming the SM value for the other cross section, respectively. Figure 1 shows a comparison of the fit results with theoretical expectations,  $\sigma_{t\bar{t}Z} = 0.88^{+0.09}_{-0.11}$  pb and  $\sigma_{t\bar{t}W} = 0.60^{+0.08}_{-0.07}$  pb [7], demonstrating good agreement between the measured and predicted cross sections. For the  $t\bar{t}Z$  process, both the observed and the expected significances are found to be much larger than 5 standard deviations. For the  $t\bar{t}W$  process, an excess of events over the expected Standard Model background-only hypothesis is found with an observed (expected) significance of 4.3 (3.4) standard deviations. Table 2 shows the uncertainties in the measured  $t\bar{t}Z$  and  $t\bar{t}W$  cross sections, grouped in categories, along with the total uncertainties. For both processes, the precision of the measurement is affected by statistical and systematic uncertainties in similar proportions. For the  $t\bar{t}Z$  determination, the dominant systematic uncertainty sources are the modelling of the backgrounds and of the signal. For the  $t\bar{t}W$  determination, the dominant systematic uncertainty sources are the modelling of the signal and the limited amount of data available in the control regions and simulated samples.

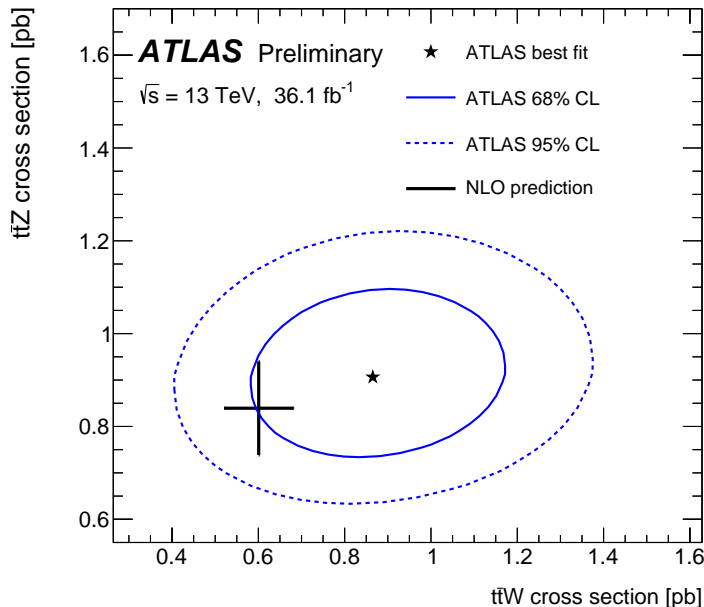


Figure 1: The result of the simultaneous fit to the  $t\bar{t}Z$  and  $t\bar{t}W$  cross sections along with the 68% and 95% confidence level (CL) contours [5]. The cross shows the theoretical uncertainties in the SM predictions, and include renormalization and factorization scale uncertainties, as well as PDF uncertainties including  $\alpha_s$  variations [7].

Table 2: List of relative uncertainties in the measured cross sections of the  $t\bar{t}Z$  and  $t\bar{t}W$  processes from the fit, grouped in categories. All uncertainties are symmetrized. The quadratic sum may not be equal to the total due to correlations between uncertainties introduced by the fit [5].

Uncertainty	$\sigma_{t\bar{t}Z}$	$\sigma_{t\bar{t}W}$
Luminosity	2.9%	4.5%
Simulated sample statistics	2.0%	5.3%
Data-driven background statistics	2.5%	6.3%
JES/JER	1.9%	4.1%
Flavor tagging	4.2%	3.7%
Other object-related	3.7%	2.5%
Data-driven background normalization	3.2%	3.9%
Modeling of backgrounds from simulation	5.3%	2.6%
Background cross sections	2.3%	4.9%
Fake leptons and charge misID	1.8%	5.7%
$t\bar{t}Z$ modelling	4.9%	0.7%
$t\bar{t}W$ modelling	0.3%	8.5%
Total systematic	10%	16%
Statistical	8.4%	15%
Total	13%	22%

## ACKNOWLEDGEMENTS

The work of the author is currently funded by the European Research Council under the European Unions Seventh Framework Programme ERC Grant Agreement n. 617185.

## References

- [1] ATLAS Collaboration, JINST **3** (2008) S08003.
- [2] CMS Collaboration, JINST **3** (2008) S08004.
- [3] ATLAS Collaboration, Eur. Phys. J. C **77** (2017), 40, arXiv:1609.01599 [hep-ex].
- [4] CMS Collaboration, JHEP **08** (2018) 011, arXiv:1711.02547 [hep-ex].
- [5] ATLAS Collaboration, ATLAS-CONF-2018-047,  
<http://cds.cern.ch/record/2639674>.
- [6] ATLAS Collaboration, Eur. Phys. J. C **71** (2011) 1577,  
arXiv:1012.1792 [hep-ex].
- [7] J. Alwall *et al.*, JHEP **07** (2014) 079, arXiv:1405.0301 [hep-ex].